Two types of type IV P-type ATPases independently re-establish the asymmetrical distribution of phosphatidylserine in plasma membranes

Yugo Miyata[1] , **Kyoko Yamada**[2], **Shigekazu Nagata**[2,*] , and **Katsumori Segawa**[1,2,*]

From the [1]*Department of Medical Chemistry, Medical Research Institute, Tokyo Medical and Dental University, Bunkyo-ku, Tokyo, Japan;* [2]*Laboratory of Biochemistry & Immunology, World Premier International Research Center, Immunology Frontier Research Center, Osaka University, Suita, Osaka, Japan*

Edited by Dennis Voelker

Phospholipids are asymmetrically distributed between the lipid bilayer of plasma membranes in which phosphatidylserine (PtdSer) is confined to the inner leaflet. ATP11A and ATP11C, type IV P-Type ATPases in plasma membranes, flip PtdSer from the outer to the inner leaflet, but involvement of other P4-ATPases is unclear. We herein demonstrated that once PtdSer was exposed on the cell surface of $ATP11A^{-/-}ATP11C^{-/-}$ mouse T cell line (W3), its internalization to the inner leaflet of plasma membranes was negligible at 15 °C. However, $ATP11A^{-/-}ATP11C^{-/-}$ cells internalized the exposed PtdSer at 37 °C, a temperature at which trafficking of intracellular membranes was active. In addition to ATP11A and 11C, W3 cells expressed ATP8A1, 8B2, 8B4, 9A, 9B, and 11B, with ATP8A1 and ATP11B being present at recycling endosomes. Cells deficient in four P4-ATPases (ATP8A1, 11A, 11B, and 11C) (QKO) did not constitutively expose PtdSer on the cell surface but lost the ability to re-establish PtdSer asymmetry within 1 hour, even at 37 °C. The expression of ATP11A or ATP11C conferred QKO cells with the ability to rapidly re-establish PtdSer asymmetry at 15 °C and 37 °C, while cells expressing ATP8A1 or ATP11B required a temperature of 37 °C to achieve this function, and a dynamin inhibitor blocked this process. These results revealed that mammalian cells are equipped with two independent mechanisms to re-establish its asymmetry: the first is a rapid process involving plasma membrane flippases, ATP11A and ATP11C, while the other is mediated by ATP8A1 and ATP11B, which require an endocytosis process.

Major glycerophospholipids in the plasma membranes of mammalian cells are phosphatidylcholine, phosphatidylethanolamine (PtdEtn), phosphatidylserine (PtdSer), phosphatidylinositol (PtdIns), and phosphatidic acid (1, 2). In addition, sphingomyelin (SM) and cholesterol are abundantly present in the plasma membrane. These lipids are asymmetrically distributed between the inner and outer leaflets of the plasma membranes. PtdSer, PtdEtn, and phosphatidylinositol are confined to the inner leaflet, whereas PtdCho and SM are enriched in the outer leaflet (3, 4).

PtdSer at the inner leaflet (or cytoplasmic side) of the plasma membrane plays an important role in the recruitment of proteins to the plasma membrane for their activation (5–7). In various biological processes, the asymmetrical distribution of PtdSer is broken, which exposes it on the cell surface (8, 9). Apoptotic cells irreversibly expose PtdSer as an "eat me" signal for macrophages (10, 11). In contrast, PtdSer is transiently and reversibly exposed by activated lymphocytes and platelets (12, 13), myoblasts and trophoblasts undergoing cell fusion (14, 15), and capacitated sperm (16), indicating the ability of mammalian cells to break and re-establish PtdSer asymmetry in the plasma membrane. The distribution of phospholipids in the lipid bilayer is regulated by flippases and scramblases (9, 17). Flippases translocate phospholipids from the outer to the cytoplasmic side of the lipid bilayer in an ATP-dependent manner, while scramblases bi-directionally pass phospholipids across the membrane in an energy-independent manner. Members of the transmembrane (TMEM)16 and XK-related family function as Ca^{2+}- and caspase-activated scramblases, respectively (18, 19).

Type IV P-type (P4-) ATPases have been proposed to function as flippases (20, 21). They carry 10 transmembrane segments and a large cytoplasmic ATPase domain. There are 14 and 15 members for human and mouse P4-ATPases, respectively, that localize at the plasma membrane, endosomes, Golgi, and lysosomes. Most of them require CDC50A as an essential subunit for their correct folding and exit from the ER. Six human P4-ATPases (ATP8A1, 8A2, 8B1, 11A, 11B, and 11C) were previously shown to exhibit PtdSer-dependent ATPase activity with purified proteins or flippase activity using a proteoliposome system (22–25). We and others demonstrated using cell-based assays that ATP8A2, 11A, and 11C localized at the plasma membrane and exhibited the ability to flip PtdSer (26, 27). On the other hand, since ATP8A1 and ATP11B localize at endomembranes, such as endosomes and the *trans*-Golgi network (TGN) (22, 28, 29), it currently remains unclear whether these intracellular P4-ATPases contribute to the asymmetrical distribution of PtdSer at the plasma membrane.

* For correspondence: Katsumori Segawa, segawa.mche@tmd.ac.jp; Shigekazu Nagata, snagata@ifrec.osaka-u.ac.jp.

Two types of P4-ATPases re-establish PtdSer asymmetry

ATP11A and ATP11C are ubiquitously expressed in various cell types, while the expression of ATP8A2 is limited to the brain or testis (23, 26). We previously reported that flippase activity at the plasma membrane of the $ATP11A^{-/-}ATP11C^{-/-}$ double flippase-deficient (DKO) mouse W3 cell line was negligible (30). In the present study, we demonstrated that after the transient exposure of PtdSer, DKO cells re-established the asymmetrical distribution of PtdSer at the plasma membrane at 37 °C, but not at 15 °C. This re-establishment activity at 37 °C was compromised by a dynamin inhibitor that blocked a clathrin-mediated endocytosis and membrane trafficking (31). When the $ATP8A1$ and $ATP11B$ genes were additionally deleted, $ATP8A1^{-/-}ATP11A^{-/-}ATP11B^{-/-}ATP11C^{-/-}$ quadruple-deficient (QKO) cells lost the ability to re-establish PtdSer asymmetry at the plasma membrane. PtdSer asymmetry was rapidly re-established in QKO cells expressing ATP11A or ATP11C, but slowly and in a temperature-dependent manner in QKO cells expressing ATP8A1 or ATP11B, and that was blocked by a dynamin inhibitor. QKO cells eventually, or within 12 h, regained plasma membrane PtdSer asymmetry at 37 °C following its exposure. This observation suggests that progression through the cell cycle allows the PtdSer asymmetry re-establishment by an unknown process that is independent of the four flippases. Accordingly, QKO cells under steady-state conditions maintained the PtdSer asymmetry in the plasma membrane. Based on these results, we concluded that mammalian cells are equipped with two types of PtdSer flippases located at the plasma membrane or endosomes that repair PtdSer asymmetry in the plasma membrane after its transient exposure.

Results

ATP11A and ATP11C are responsible for flipping PtdSer on the cell surface

We previously reported that W3 cells, a mouse T-lymphoma cell line, expressed eight P4-ATPases (ATP8A1, 8B2, 8B4, 9A, 9B, 11A, 11B, and 11C) (32), while $ATP11A-ATP11C$ DKO cells lost PtdSer flippase activity at the plasma membrane (26, 30). Plasma membrane flippases can be assessed using the fluorescent-labeled PtdSer analog, 1-oleoyl-2-{6-[(7-nitro-2–1,3-benzoxadiazol-4-yl)amino]hexanoyl}-sn-glycero-3-phosphoserine (NBD-PS) (see Experimental procedures). We initially investigated the time course and effects of temperature on flippase activity. As shown in Fig. 1A, WT-W3 cells efficiently flipped NBD-PS into the inner leaflet at 15 °C, and its median fluorescence intensity (MFI) increased at least for 6 min. PtdSer-flipping kinetics were accelerated at 37 °C, reaching a plateau by 3 min. In contrast, a time-dependent increase in MFI was not observed in DKO cells at 15 °C or 37 °C, indicating that PtdSer flippase activity on the cell surface of DKO cells was negligible. We then examined endogenous PtdSer distribution on the cell surface with annexin V, a PtdSer-binding protein, and found that they did not expose PtdSer despite the loss of PtdSer flippase activity (Fig. 1B). By contrast, when W3 and DKO cells were treated with a calcium ionophore A23187, they exposed PtdSer on the cell surface within 5 min through the activation of the calcium-dependent scramblase, TMEM16F (18). This result indicated that the asymmetrical distribution of PtdSer on the cell surface was established without plasma membrane flippases or was mediated by intracellular mechanisms.

ATP11A- and ATP11C-independent systems to re-establish the asymmetrical distribution of PtdSer in plasma membranes

We then investigated the process to re-establish the asymmetrical distribution of endogenous PtdSer after the transient exposure of PtdSer caused by A23187 treatment. Once the ionophore was removed from the culture medium, W3 cells rapidly flipped exposed PtdSer into the inner leaflet of the plasma membrane at both 15 °C and 37 °C (Fig. 2, A and B). Within 4 min ($t_{1/2}$, 4 min), half of the population internalized PtdSer. In
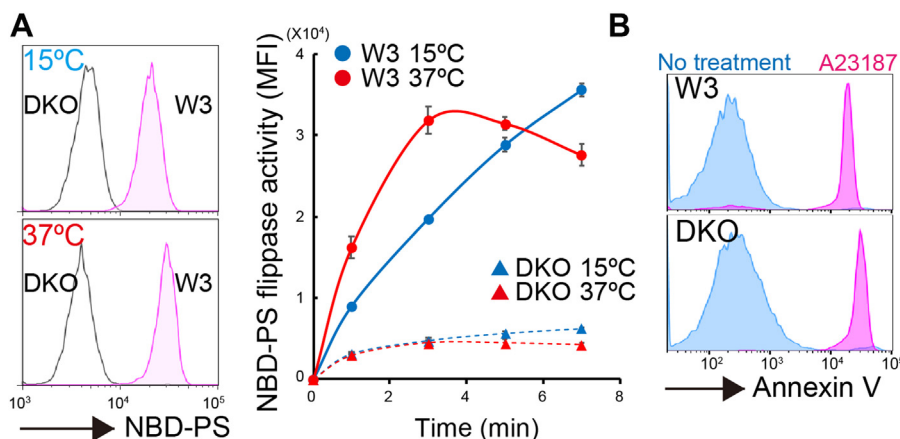

Figure 1. Requirement of ATP11A and ATP11C to flip PtdSer at the plasma membrane. *A*, PtdSer-flippase activity at the plasma membrane. W3 and $ATP11A^{-/-}ATP11C^{-/-}$ W3 (DKO) cells were incubated with 0.5 μM NBD-PS at 15 or 37 °C for 3 min (*left*) or the indicated time (*right*), and the internalization of NBD-PS was measured by flow cytometry. Representative FACS histograms for NBD-PS and the time course for NBD-PS internalization are shown (*left*). The experiment was repeated three times and the average median fluorescence intensity (MFI) was plotted with SD (*bar*) (*right*). *B*, PtdSer-exposure on the cell surface. W3 and DKO cells before (*blue*) or after the treatment of 3 μM ionophore at 30 °C for 5 min (*magenta*) were stained with Cy5-annexin V in the presence of propidium iodide (PI) and analyzed by flow cytometry. Representative histograms for annexin V in the PI-negative populations are shown. PtdSer, phosphatidylserine; NBD-PS, 1-oleoyl-2-{6-[(7-nitro-2–1,3-benzoxadiazol-4-yl)amino]hexanoyl}-sn-glycero-3-phosphoserine.
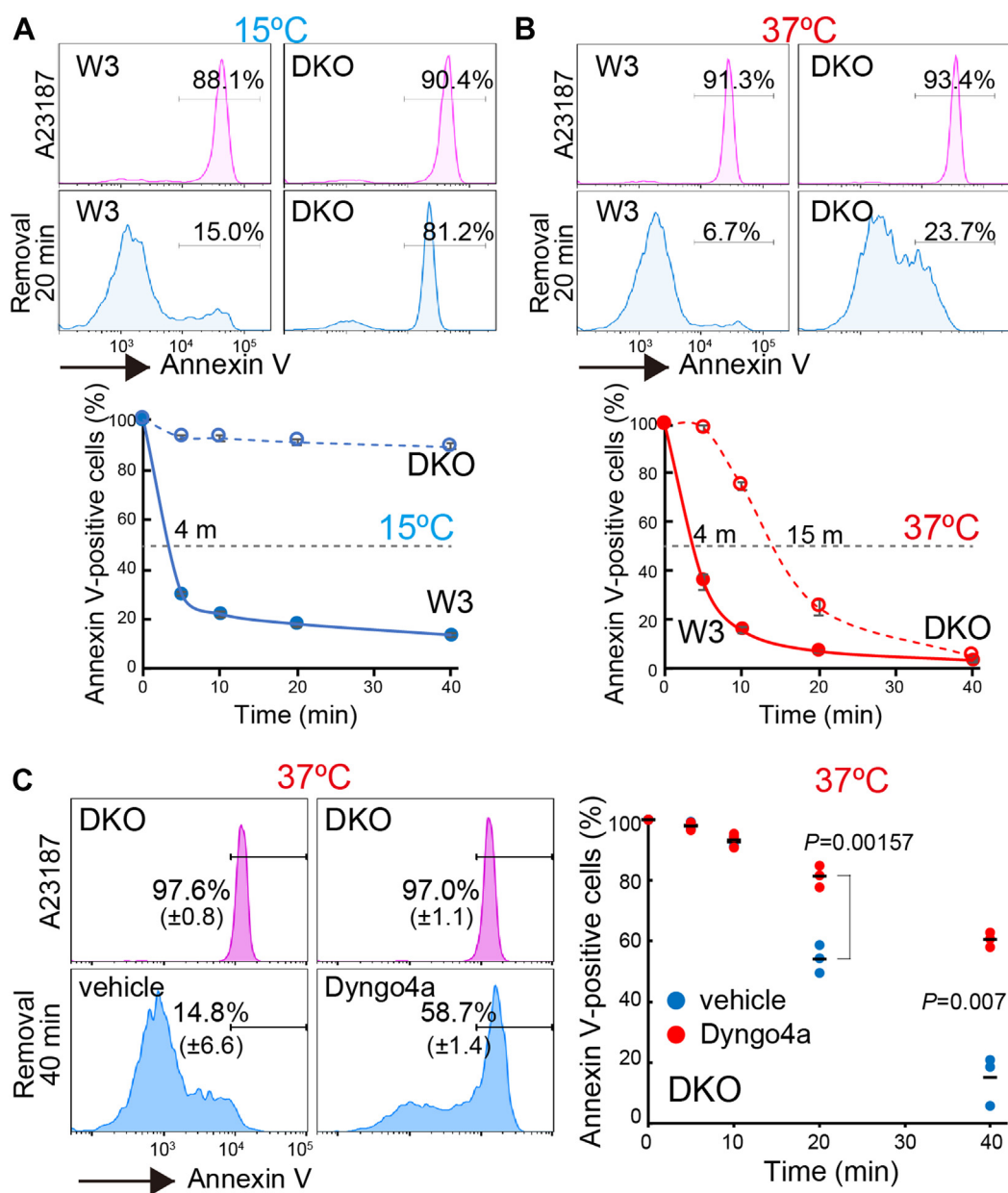
Figure 2. Temperature- and dynamin-dependent re-establishment activity of PtdSer asymmetry in DKO cells. *A–C*, W3 and DKO cells were stimulated with A23187 at 30 °C for 5 min. After removing A23187, cells were incubated in RPMI-10% FCS with 2 mM EGTA in the presence or absence of 25 μM Dyngo-4a for the indicated time at 15 °C (*A*) or 37 °C (*B* and *C*). Cells were then stained with Cy5-annexin V and analyzed by flow cytometry. Annexin V-positive cells in the PI-negative population at the indicated time are expressed as the percentage of that found in cells after the A23187 stimulation (*A, bottom; B, bottom*; and *C, right*). The experiment was repeated two or three times and average values were plotted with SD (*bar*). The times required to reduce the PS-exposing cell population by 50% are shown. The histograms show representative annexin V profiles of cells treated with A23187 (*magenta*) and cells that were chased in the presence of 2 mM EGTA at 15 °C or 37 °C for 20 min (*blue*) (*A* and *B; top*), or in the presence or absence of 25 μM Dyngo-4a at 37 °C for 40 min (*blue*) (*C; left*). *p* values are shown. DKO, *ATP11A^{−/−}ATP11C^{−/−}* double flippase-deficient; PI, propidium iodide; PtdSer, phosphatidylserine.

contrast, DKO cells lost the ability to flip exposed PtdSer at 15 °C, keeping it on the cell surface (Fig. 2*A*). This result indicated that ATP11A and ATP11C are essential for re-establishing PtdSer asymmetry at 15 °C. However, following an increase in temperature to 37 °C, DKO cells slowly internalized PtdSer from the surface ($t_{1/2}$, 15 min), and PtdSer on DKO cells disappeared within 40 min, re-establishing PtdSer asymmetry (Fig. 2*B*). These results indicated that DKO cells exhibit a temperature-dependent activity to re-establish the asymmetrical distribution of PtdSer.

Endocytosis and intracellular membrane trafficking are active at 37 °C and blocked at 15 °C (33, 34). Accordingly,

when W3 cells were treated with pH-sensitive fluorescent-conjugated transferrin (pHrodo-Transferrin) at 37 °C, it was quickly incorporated into cells and showed intracellular puncta signals (Fig. S1, *A* and *B*). This process was blocked at 15 °C or by Dyngo-4a, a dynamin inhibitor, that blocks the clathrin-mediated endocytosis or membrane trafficking (31) (Fig. S1, *B* and *C*), confirming that W3 cells have normal endocytosis and membrane trafficking systems. We speculated that intracellular P4-ATPases support the re-establishment of the asymmetrical distribution of PtdSer at the plasma membrane through temperature-dependent membrane trafficking

systems. Accordingly, Dyngo-4a inhibited DKO cell's activity to re-establish PtdSer asymmetry at 37 °C in a time- and concentration-dependent manner (Figs. 2*C* and S1*D*).

ATP8A1 and ATP11B, intracellular P4-ATPases, re-establish PtdSer asymmetry in a temperature- and membrane trafficking-dependent manner

Six mammalian P4-ATPases have been shown to exhibit PtdSer flippase activity (22–27), and ATP8A1 and ATP11B localize at endosomes or the *trans*-Golgi network. Therefore, we examined the effects of ATP8A1 and ATP11B on the re-establishment of the asymmetrical distribution of PtdSer in DKO cells. The *ATP8A1* and/or *ATP11B* genes on DKO cells were knocked out using CRISPR-Cas9 technology (Fig. S2),

establishing *ATP11A-ATP11C-ATP8A1* (DKO-*ATP8A1*$^{-/-}$: TKO1) and *ATP11A-ATP11C-ATP11B* (DKO-*ATP11B*$^{-/-}$: TKO2) triple flippase-deficient, and *ATP11A-ATP11C-ATP8A1-ATP11B* QKO cells. QKO cells grew as well as WT cells and did not exhibit abnormalities under steady-state conditions (Fig. 3*A*). As shown in Fig. 3*B*, PtdSer flippase activity using NBD-PS at the plasma membrane did not substantially differ between DKO and QKO cells at 15 °C or 37 °C, indicating that ATP8A1 and ATP11B did not contribute to this process. In contrast, the re-establishment of PtdSer asymmetry by these cells at 37 °C after the transient exposure of PtdSer was totally different. As shown in Fig. 3*C*, the half time required for this process increased from 22 min with DKO cells to 33 and 52 min with TKO1 and TKO2 cells, respectively, and the re-establishment activity of DKO cells
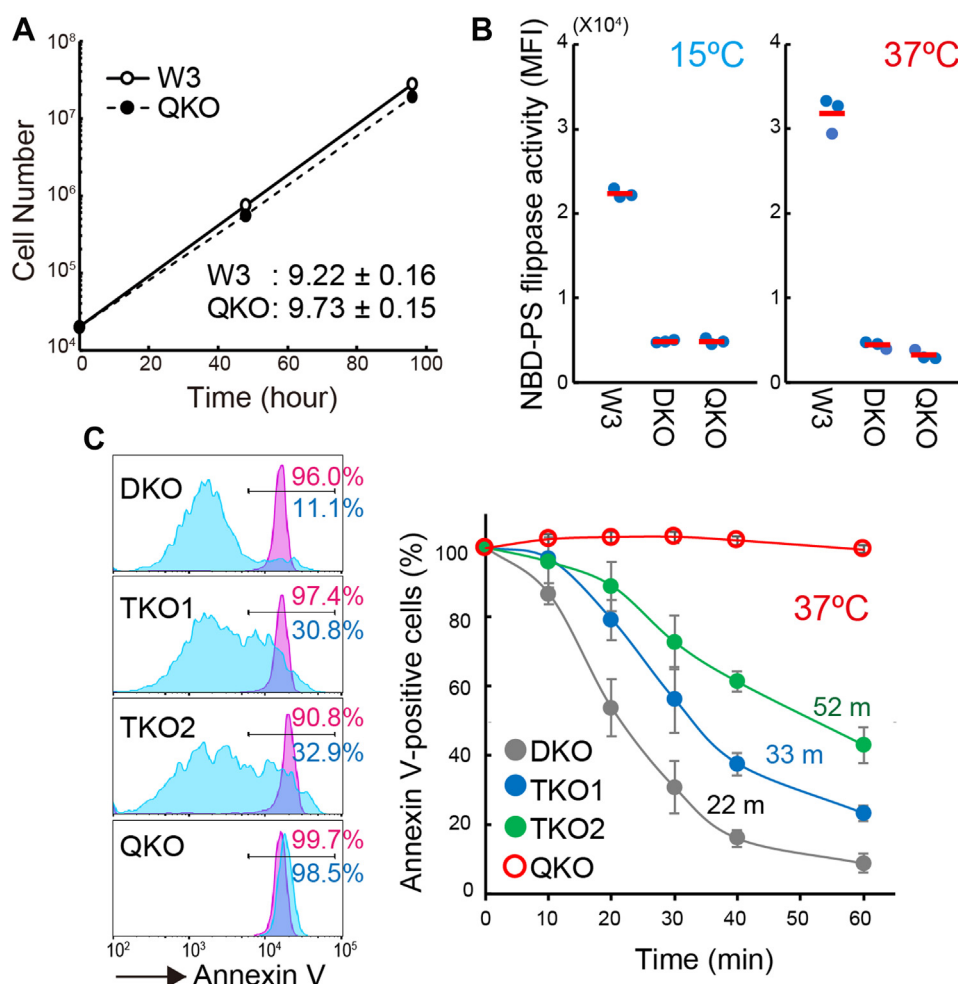

Figure 3. Essential roles of ATP8A1 and ATP11B for the temperature-dependent re-establishment of PtdSer asymmetry. *A*, W3 or QKO cells were cultured for 2 days and re-seeded at 2×10^4 cells/ml. Viable cells were counted after staining with *trypan blue*, and average cell numbers were plotted. Experiments were performed in triplicate, and average cell numbers were plotted. The doubling times for W3 and QKO cells are shown with SD. *B*, PtdSer-flippase activity at the plasma membrane. W3, *ATP11A*$^{-/-}$*ATP11C*$^{-/-}$ (DKO), and *ATP11A*$^{-/-}$*ATP11C*$^{-/-}$*ATP8A1*$^{-/-}$*ATP11B*$^{-/-}$ (QKO) cells were incubated with 0.5 μM NBD-PS at 15 °C or 37 °C for 5 min and analyzed by flow cytometry. The experiment was repeated three times and the MFI value was plotted, and *red bars* indicate the average values. *C*, requirement of ATP8A1 and ATP11B for the temperature-dependent re-establishment of the asymmetrical distribution of PtdSer. After a treatment with 3 μM A23187 at 30 °C for 5 min, DKO, DKO-*ATP8A1*$^{-/-}$ (TKO1), DKO-*ATP11B*$^{-/-}$ (TKO2), and QKO cells were incubated at 37 °C for the indicated periods in the presence of 2 mM EGTA, stained with Cy5-annexin V and PI, and analyzed by flow cytometry. Annexin V-positive cells in the PI-negative population are expressed as a percentage of that present before the EGTA treatment (*right*). The experiment was repeated three times and average values were plotted with SD (*bar*). The times required to reduce the PS-exposing cell population by 50% are shown. *Left* panels show representative annexin V-staining profiles before (*magenta*) and after a 40-min incubation with EGTA (*blue*). DKO, *ATP11A*$^{-/-}$*ATP11C*$^{-/-}$ double flippase-deficient; MFI, median fluorescence intensity; NBD-PS, 1-oleoyl-2-{6-[(7-nitro-2–1,3-benzoxadiazol-4-yl)amino]hexanoyl}-sn-glycero-3-phosphoserine; PI, propidium iodide; PtdSer, phosphatidylserine.

was abolished entirely in QKO cells. Gene deletion of ATP11B impacted stronger on the re-establishment activity than ATP8A1, which may be consistent with abundant mRNA expressions of ATP11B in W3 cells (32). The robust exposure of PtdSer on QKO cells was maintained at 37 °C for 60 min. These results indicated that the four P4-ATPases (ATP8A1, ATP11A, ATP11B, and ATP11C) were involved in re-establishing PtdSer asymmetry in W3 cells.

To examine how each member contributes to the process, they were tagged with EGFP and individually expressed in QKO cells and observed with confocal microscopy or analyzed by Western blotting with anti-GFP Ab. As shown in Figs. 4*A* and S3, EGFP-ATP11A and ATP11C were exclusively merged

with PlasMem Bright that specifically stains the plasma membrane (35). On the other hand, consistent with previous findings (22, 28), majority of the GFP signals of EGFP-tagged ATP8A1 and ATP11B were merged with pHrodo-Transferrin (Fig. 4*B*) in recycling endosomes (36) and partly colocalized with PlasMem Bright. The expression of ATP11A and ATP11C conferred rapid activity to re-establish PtdSer asymmetry in QKO cells after the exposure of PtdSer, which was not affected by temperature (Fig. 4*C*). On the other hand, ATP8A1 and ATP11B internalized PtdSer as efficiently as ATP11A or ATP11C at 37 °C, but less efficiently at 15 °C. Approximately 25% of QKO expressing ATP8A1 cells internalized PtdSer quickly at 15 °C, which may be consistent with
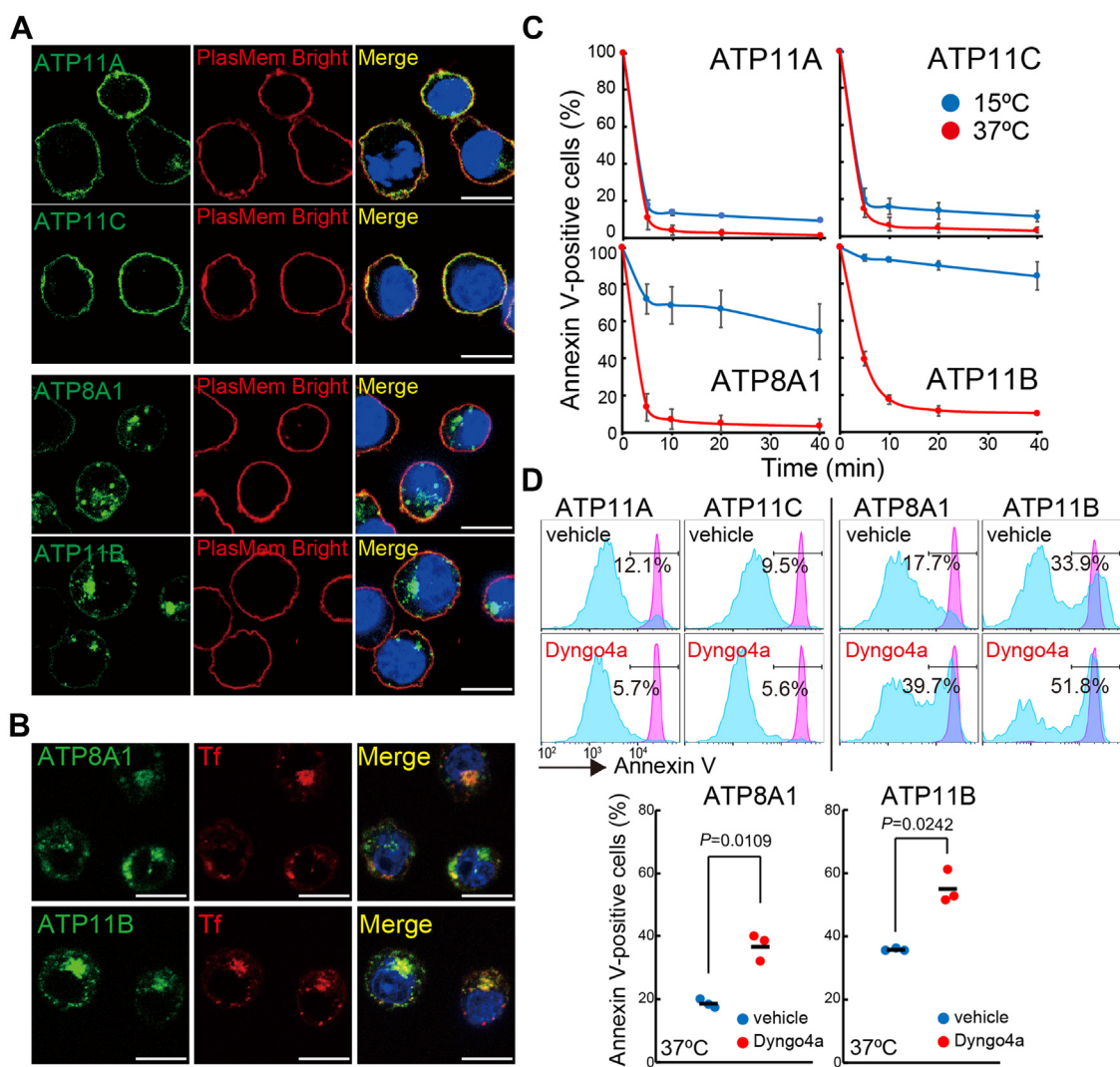

Figure 4. ATP8A1 and ATP11B re-establish PtdSer asymmetry in a temperature- and dynamin-dependent manner. *A* and *B*, EGFP-tagged ATP8A1, ATP11A, ATP11B, or ATP11C was stably expressed in QKO cells and observed under a confocal microscope. Images show EGFP (*green*, *A* and *B*), PlasMem Bright (*red*, *A*), pHrodo-Transferrin (Tf) (*red*, *B*), Hoechst 33342 (*blue*, *A* and *B*), and merged images (*A* and *B*). Bar, 10 μm. *C*, QKO transformants expressing ATP8A1, 11A, 11B, or 11C were treated with A23187, and incubated in the presence of 2 mM EGTA for the indicated time at 15 °C (*blue*) or 37 °C (*red*). Annexin V-positive cells in the PI-negative populations are expressed as a percentage of that present before the EGTA treatment. The experiment was repeated three times, and average values were plotted with SD (*bar*). *D*, QKO transformants were stimulated by A23187 as above and allowed to internalize PtdSer in the presence or absence of 25 μM Dyngo-4a at 37 °C for 15 min (ATP11A and 11C) (*top left*) and 40 min (ATP8A1 and 11B) (*top right* and *bottom*). *Top* panels show representative annexin V profiles of cells treated with A23187 (*red*) and cells that were further incubated in the presence or absence of 25 μM Dyngo-4a (*blue*). The percentages of cells with annexin V-positive in the PI-negative populations after the recovery are shown in the histograms. In *bottom*, annexin V-positive QKO cells expressing ATP8A1 or ATP11B after the recovery procedure with or without 25 μM Dyngo-4a are expressed as a percentage of that present just after A23187 treatment and plotted (n = 3). *p* values are shown. QKO, *ATP8A1$^{-/-}$ATP11A$^{-/-}$ATP11B$^{-/-}$ATP11C$^{-/-}$* quadruple-deficient; PI, propidium iodide; PtdSer, phosphatidylserine.

SASBMB

J. Biol. Chem. (2022) 298(11) 102527 **5**

the partial localization of ATP8A1 at plasma membranes (Fig. 4A). Although Dyngo-4a did not affect the quick re-establishment of PtdSer asymmetry by ATP11A or ATP11C at 37 °C (Fig. 4D), it interfered in the ATP8A1- or ATP11B-mediated re-establishment processes. Based on these results, we concluded that in contrast to ATP11A and ATP11C, which function at the plasma membrane, the ability of ATP8A1 and ATP11B to re-establish PtdSer asymmetry was dependent on a dynamin-mediated endocytosis or recycling systems between endosomes and plasma membranes.

PtdSer-dependent ATPase activities of ATP8A1 and ATP11B

We previously showed that PtdSer triggered the ATPase activity of ATP11A and ATP11C with half-maximum activation constants (K_a) and V_{max} of 1.9 μM and 6.5 nmol Pi/μg protein/min, and 1.3 μM and 8.9 nmol Pi/μg protein/min, respectively (26). On the other hand, Wang *et al.* (23) recently reported that the K_a and V_{max} of human ATP11B for PtdSer were 178 μM and 17.3 nmol Pi/μg protein/min, respectively. Therefore, we investigated the PtdSer-dependent ATPase

activity of the purified ATP8A1-CDC50A and ATP11B-CDC50A flippase complex and compared it with that of ATP11C-CDC50A, a plasma membrane PtdSer-flippase. Human ATP8A1, ATP11B, and ATP11C were tagged with FLAG and expressed in HEK293T cells with their human CDC50A subunit tagged with EGFP. Cells were lysed with 0.5% lauryl maltose-neopentyl glycol (LMNG), and the complex was affinity-purified with an anti-FLAG mAb, as previously reported (37). An analysis by SDS-PAGE followed by Coomassie Brilliant Blue (CBB) staining indicated that recombinant ATP8A1, ATP11B, and ATP11C in the complex had the expected sizes of M_r, 110K–120K (Fig. 5A). CDC50A was detected in several bands at M_r of approximately 60 to 75K, which may have been due to different degrees of glycosylation. An analysis by Blue Native-PAGE (BN-PAGE) followed by CBB staining or Western blotting with anti-FLAG (P4-ATPase) and anti-GFP (CDC50A) antibodies (Abs) detected a protein complex at approximately 300 to 450 kDa (Fig. 5, B and C).

POPS induced the ATPase activity of these complexes in a concentration-dependent manner (Fig. 5D). The complexes
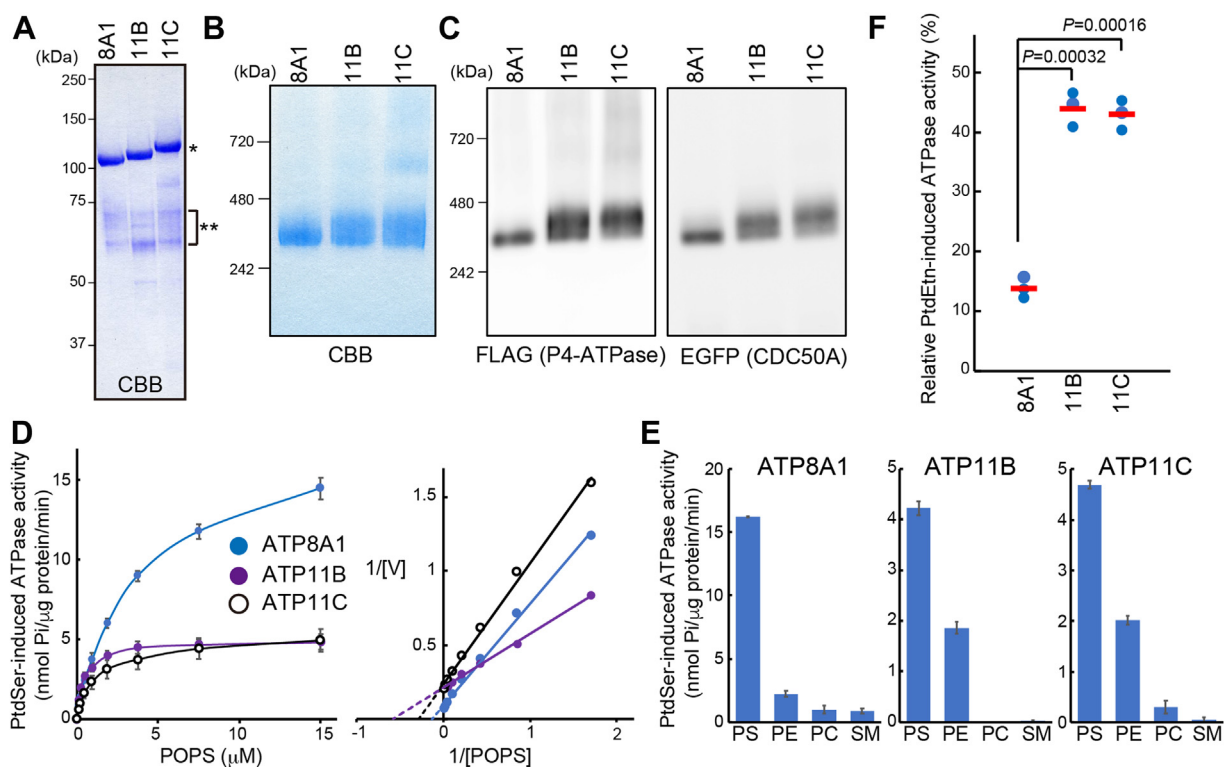

Figure 5. ATPase activities of intracellular P4-ATPases. *A–C*, analysis of purified flippase complexes by SDS-PAGE (*A*) or BN-PAGE (*B* and *C*). Flag-tagged hATP8A1, ATP11A, or ATP11C was expressed in HEK293T cells together with EGFP-tagged hCDC50A and purified. In *A*, the purified protein (300–500 ng) was separated by SDS-PAGE and stained by Coomassie Brilliant Blue (CBB). *Asterisks* indicate P4-ATPase (*) and CDC50A (**). In *B* and *C*, proteins (5–15 ng for Western blotting and 900 ng for CBB staining) were separated by BN-PAGE. Proteins were then stained by CBB or analyzed by Western blotting with an anti-FLAG or anti-GFP Ab. *D*, PtdSer-dependent ATPase activity. The ATPase activity (nmol Pi/μg protein/min) of the purified flippase complex was assessed in the presence of the indicated concentrations of POPS. ATPase activity observed without POPS was subtracted. The experiment was performed three times, and mean values were plotted with SD (*bar*). The right panel shows Lineweaver–Burk plots for PtdSer. The calculated maximal reaction rate (V_{max}) and PtdSer half-maximum activation constant (K_a) were as follows: hATP8A1; V_{max} = 11.2 nmol Pi/μg protein/min, K_a = 1.5 μM, hATP11B; V_{max} = 4.8 nmol Pi/μg protein/min, K_a = 0.4 μM, hATP11C; V_{max} = 4.3 nmol Pi/μg protein/min, K_a = 0.7 μM. *E*, lipid-induced ATPase activity was assessed at a concentration of 30 μM of the indicated lipids. ATPase activity observed without lipids was subtracted. The experiment was performed three times, and mean values were plotted with SD (*bar*). PS: POPS, PE: POPE, PC: POPC, SM: sphingomyelin (d18:1/18:0). *F*, relative PtdEtn-induced ATPase activity is shown as a percentage of respective POPS-induced ATPase activity with mean values (*bar*) (n = 3). *p* values are shown. BN-PAGE, Blue Native-PAGE; POPE, 1-palmitoyl-2-oleoyl-sn-glycero-3-phosphoethanolamine; POPS, 1-palmitoyl-2-oleoyl-sn-glycero-3-phospho-L-serine; P4-ATPase, type IV P-type ATPase; P4-ATPase, type IV P-type ATPase; PtdEtn, phosphatidylethanolamine; PtdSer, phosphatidylserine.

responded weakly to POPE, but not to POPC or SM for ATPase activity (Fig. 5E). POPE induced the ATPase activity of ATP11B and ATP11C with approximately 40% efficiency of POPS, while it activated the ATPase of ATP8A1 with around 13% of POPS, suggesting that ATP11B and ATP11C responded better to PtdEtn than ATP8A1 (Fig. 5F). A Lineweaver–Burk kinetics analysis indicated that K_a for POPS was similar among the three P4-ATPases (ATP8A1, ATP11B, and ATP11C): K_a of 0.4 to 1.5 μM, whereas V_{max} of ATP8A1 for POPS was three-times higher than those of ATP11B and ATP11C (11.2, 4.8, and 4.3 nmol Pi/μg protein/min, respectively). These results were consistent with the values we previously reported for the recombinant human ATP11A and ATP11C flippase complexes (26), supporting ATP8A1 and ATP11B functions at endosomes as flippases for PtdSer. On the other hand, K_a values were approximately 100- to 400-fold smaller than those reported by Wang *et al.* (23). Although we do not have a clear explanation for this difference, it may be due to the presence or absence of a high concentration of detergents in the assay (10 mM CHAPS in (23) or 0.5 mM LMNG in this study).

No PtdSer exposure on QKO cells that lack flippases at the plasma membrane and endosomes

We and others previously reported that the loss of CDC50A caused the constitutive exposure of PtdSer in W3 and various types of cells (32, 38–40). Accordingly, *CDC50A*-null W3 cells firmly bound annexin V under steady-state conditions (Fig. 6A). W3 cells expressed eight out of 14 P4-ATPases (ATP8A1, 8B2, 8B4, 9A, 9B, 11A, 11B, and 11C). Although ATP8B2 and 8B4 are present in the plasma membrane, they do not exhibit flippase activity for PtdSer or any other potential substrates tested in a cell-based assay using fluorescent-conjugated phospholipid analogs (26). In addition, ATP9A and ATP9B do not form complexes with CDC50A and do not require CDC50A for their proper cellular localization (28). Therefore, we expected QKO cells lacking ATP8A1, 11A, 11B, and 11C to exhibit similar behavior to *CDC50A*-null cells and constitutively expose PtdSer. However, the level of PtdSer exposed on the surface of QKO cells was very low at approximately 10 to 20% of that in *CDC50A*-null cells (Fig. 6A). These results indicated the presence of another CDC50A-dependent system that constitutively establishes the asymmetrical distribution of PtdSer.
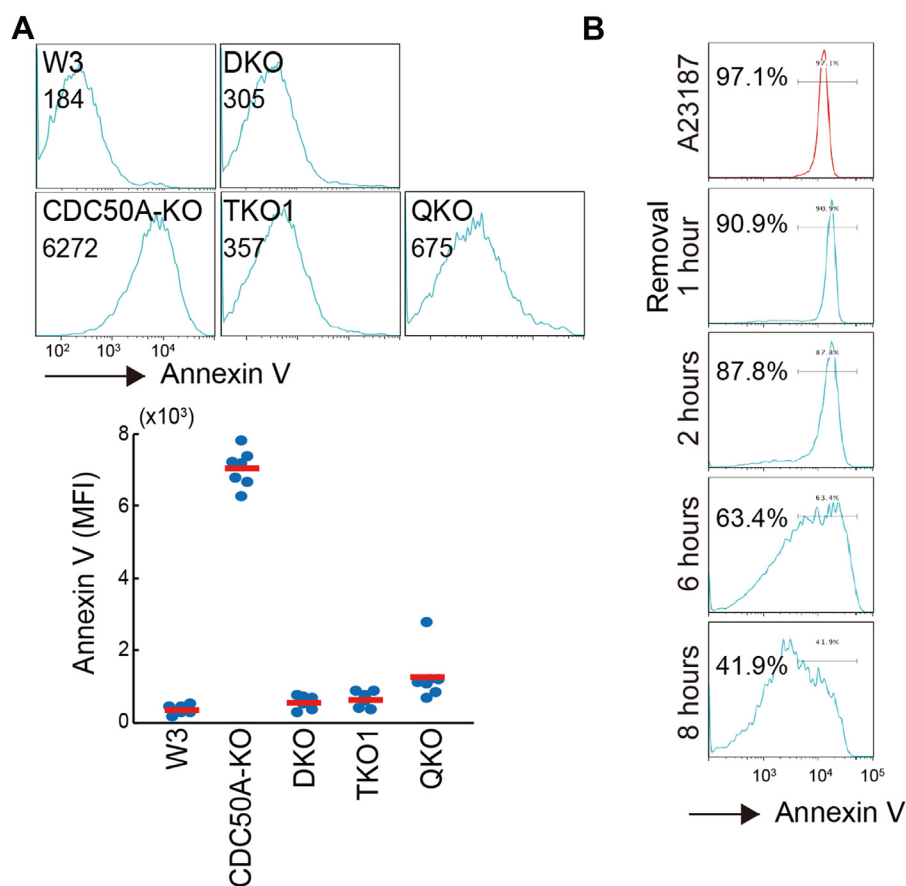

Figure 6. Establishment of the asymmetrical distribution of PtdSer in the plasma membrane of QKO cells under steady-state conditions. *A*, the asymmetrical distribution of PtdSer in the plasma membrane. The indicated cells were stained with Cy5-conjugated annexin V in the presence of PI and analyzed by flow cytometry. Representative histograms for annexin V staining in the PI-negative population with MFI values (*top*). Experiments were performed seven times, and MFI values were plotted with the average value (*red bar*). *B*, QKO cells were stimulated with A23187 for 5 min (*red*). After a treatment with 3 μM A23187 at 30 °C for 5 min, QKO cells were incubated at 37 °C for the indicated periods in RPMI-10%FCS containing 1 mM MgCl₂, stained with Cy5-annexin V and PI, and analyzed by flow cytometry. Annexin V-positive cells in the PI-negative population are expressed as a percentage in the total PI-negative population. QKO, *ATP8A1⁻/⁻ATP11A⁻/⁻ATP11B⁻/⁻ATP11C⁻/⁻* quadruple-deficient; MFI, median fluorescence intensity; PI, propidium iodide; PtdSer, phosphatidylserine.

Two types of P4-ATPases re-establish PtdSer asymmetry

To further characterize this system, we followed the establishment of PtdSer asymmetry for a long time. As shown in Fig. 6B, most QKO cells (97.1%) became annexin V-positive when treated with a calcium-ionophore. QKO cells continued to expose PtdSer at 37 °C for 2 h after the removal of the ionophore. However, cells with asymmetrically distributed PtdSer started to appear after a 6-h chase period. More than 55% of cells lost the ability to bind annexin V after 8 h. QKO cells, similar to WT-W3 cells, grew with a doubling time of 9.7 h (Fig. 3A), suggesting that the disappearance of PtdSer from the cell surface in QKO cells may be coupled with cell division.

Discussion

The plasma membranes of eukaryote cells comprise a lipid bilayer, and PtdSer exclusively localizes at the inner leaflet. In the present study, we used a mouse T cell lymphoma and identified two independent systems establishing the asymmetrical distribution of PtdSer. The first system is mediated by two P4-ATPases, ATP11A and ATP11C, which translocate PtdSer from the outer leaflet to the inner leaflet in the plasma membrane. This system is rapid (within 5 min) and appears to take place with no involvement of intracellular components. Another pathway requires ATP8A1 or ATP11B, other P4-ATPases that localize in endosomes. This system is slower than the first system (within 60 min) and requires a temperature of 37 °C. Since a dynamin inhibitor blocked the process, ATP8A1 and ATP11B most likely required a dynamin-mediated process such as clathrin-mediated endocytosis and recycling of endosomal components to create PtdSer asymmetry in the plasma membrane.

Eukaryotic cells carry multiple P4-ATPase genes, and the number of P4-ATPase family members has increased with organismal complexity during evolution; yeast, *Caenorhabditis elegans*, and the human genome encode 5, 6, and 14 genes, respectively (21, 41). In the present study, we showed that among 14 human P4-ATPases, at least four, either in the plasma membrane or endosomes, were involved in establishing the asymmetrical distribution of PtdSer in the plasma membrane. These four P4-ATPases (ATP8A1, ATP11A, ATP11B, and ATP11C) are broadly expressed in mice and humans (23, 26) (The human protein atlas: https://www.proteinatlas.org) and, thus, redundantly support PtdSer asymmetry at the plasma membrane in most cell types. This result appears to provide support for multiple P4-ATPases redundantly contributing to the asymmetrical distribution of phospholipids at the plasma membrane in yeasts (42, 43). On the other hand, a loss-of-function mutation in ATP11A and ATP11C, but not in ATP8A1 or ATP11B, causes severe phenotypes in mice and humans due to their limited exclusive expression in some cell types (44–48) (The International Mouse Phenotyping Consortium: https://www.mousephenotype.org). These results indicate that ATP11A and ATP11C play a major role in maintaining the asymmetrical distribution of PtdSer at the plasma membrane, and ATP8A1 and ATP11B function as backup systems. Further studies are warranted to establish

mouse mutants lacking the ATP8A1 and 11B systems in order to investigate the physiological role of flippases at endosomes and their backup functions for PtdSer asymmetry in plasma membranes.

ATP8A1 and ATP11C have a similar tertiary structure and are likely to translocate PtdSer in the lipid bilayer with a similar mechanism (49, 50). The mechanisms by which ATP8A1 and ATP11B in endosomes regulate the distribution of PtdSer at the plasma membrane currently remain unclear. We propose two mechanisms. In the first mechanism, ATP8A1 and ATP11B are recycled between the endosomes and plasma membranes as in the case of lipoprotein or cytokine receptors (51). These flippases may transiently move to the plasma membrane to flip PtdSer and return to the endosomes. The other mechanism involves ATP8A1 and ATP11B functioning as flippases at endosomes, with endosomal recycling systems or lipid exchange systems, such as ORP5 and ORP8, transferring PtdSer from endosomes to the plasma membrane (52). It will be necessary to examine whether ATP8A1 and ATP11B recycle between the plasma membrane and endosomes during the re-establishment processes after PtdSer exposure.

We and others previously reported that *CDC50A*-null mutation causes the constitutive PtdSer-exposure in various cell types (32, 38–40). CDC50A is an essential subunit for P4-ATPase family members (ATP8A1, 8A2, 8B1–8B4, 10A, 10B, 10D, and 11A–11C), except for ATP9A and ATP9B (26, 28). Although QKO cells lack the CDC50A-dependent PtdSer flippases expressed on the plasma membrane, they did not expose PtdSer on the cell surface. In addition to the four P4-ATPases (ATP8A1, 11A, 11B, and 11C), W3 cells express ATP8B2 and ATP8B4, and these P4-ATPases may contribute to the asymmetrical distribution of PtdSer in QKO cells. Another possible explanation for this difference is that CDC50A binds and regulates other molecules that do not belong to the P4-ATPase family but is involved in establishing PtdSer asymmetry in the plasma membrane. It is important to note that Wang *et al*. applied affinity purification with mAb against CDC50A in mouse tissues and demonstrated that several proteins other than P4-ATPases formed a complex with CDC50A (23). Some of these proteins may contribute to the establishment of PtdSer asymmetry in the plasma membrane in a CDC50A-dependent manner.

We showed that QKO cells under steady-state conditions had plasma membranes in which PtdSer was asymmetrically distributed between the two leaflets. PtdSer exposed on the surface of QKO cells by stimulation with the calcium ionophore eventually disappeared from the surface with a half-life of 8 h. The time required for the disappearance of PtdSer was close to the doubling time of QKO cells. The area of the plasma membrane is doubled for cell division. The scramblase activated by the calcium ionophore is most likely to cause a 1:1 distribution of PtdSer between the outer and inner leaflets of the plasma membrane. The mechanisms by which QKO cells re-organized the PtdSer asymmetry when cells divide were unclear. As discussed above, the remaining CDC50A-dependent P4-ATPases (ATP8B2 and 8B4) or other

CDC50A-partners may contribute to this process. Alternatively, it may be because PtdSer synthesized in the cytoplasmic leaflet of ER goes to the inner leaflet of the plasma membrane *via* a vesicular transport system or lipid transfer protein (7, 53). The molecular mechanisms by which the plasma membrane is formed during cell division have not yet been elucidated in detail (54, 55). QKO cells, in which cell division appears to play an important role in establishing asymmetrical PtdSer distribution, may be useful for investigating this process.

Experimental procedures

Cell lines, plasmids, Abs, and reagents

Human HEK293T cells (ATCC; CRL-1573) were cultured in Dulbecco's modified Eagle's medium containing 10% Fetal Calf Serum (FCS). W3 is a mouse T cell lymphoma (WR19L; ATCC TIB52) expressing mouse Fas (56), and was cultured in RPMI 1640 supplemented with 10% fetal calf serum. The $ATP11A^{-/-}ATP11C^{-/-}$ (DKO) and $CDC50A^{-/-}$ W3 lines were previously described (30, 37, 46). $ATP8A1^{-/-}ATP11A^{-/-}ATP11C^{-/-}$ TKO1, $ATP11A^{-/-}ATP11B^{-/-}ATP11C^{-/-}$ TKO2, and $ATP8A1^{-/-}ATP11A^{-/-}ATP11B^{-/-}ATP11C^{-/-}$ QKO W3 mutant cell lines were established from DKO cells by a CRISPR-Cas9 system using the pX330 vector (57). In brief, DKO cells were electroporated with the pX330 vector carrying the following sequence to produce sgRNA for *ATP8A1* and *ATP11B*. *ATP8A1*, 5′-CACC-GAGTGTTGTGTAACGACCGGT-3′ and 5′-AAACACCGG TCGTTACACAACACTC-3′; *ATP11B*, 5′-CACCGAATGTT-CAAACTGACGGCAT-3′and 5′-AAACATGCCGTCAGTT TGAACATTC-3′. Target sequences are underlined. Gene-editing at targeted loci was verified by Sanger sequencing (Fig. S2).

The pMXs-puro retroviral vector and pGag-pol-IRES-bsr packaging plasmid (58) were from T. Kitamura (Institute of Medical Science, University of Tokyo). The pCMV-VSV-G plasmid was from H. Miyoshi (Riken Bioresource Center). pAdVAntage was purchased from Thermo Fisher Scientific. Human cDNAs for *CDC50A* (NM_018247.3), *ATP8A1* (NM_001105529.1), *ATP11A* (NM_015205.2), *ATP11B* (NM_014616.3), and *ATP11C* (XM_005262405.1) were previously described (26). cDNAs were tagged with FLAG or EGFP at the C terminus, introduced into pMXs-puro or pEF-BOS-Ex (59), and used to transform W3 or produce recombinant proteins in HEK293T cells, respectively.

A horseradish peroxidase (HRP)-conjugated rabbit anti-GFP Ab was purchased from Medical & Biological Laboratories. An HRP-conjugated anti-FLAG M2 mAb and anti-FLAG M2-conjugated magnetic beads were from Sigma-Aldrich. Hoechst 33342 and PlasMem Bright Red, and pHrodo Red-Transferrin conjugates were from Dojindo and Thermo Fisher Scientific, respectively. NBD-PS, 1-palmitoyl- 2-oleoyl-sn-glycero-3 -phospho-L-serine (POPS), 1-palmitoyl-2-oleoyl-*sn*-glycero-3- phosphoethanolamine (POPE), 1-palmitoyl-2- oleoyl-*sn*-glycero-3-phosphocholine (POPC), and N-stearoyl-D- *erythro*-sphingosylphosphorylcholine (SM) were purchased from Avanti Polar Lipids. Polyethylenimine

was from Polysciences. A23187 and Dyngo-4a were from abcam.

Cell transformation

The transformation of W3 cells was performed as previously described (26). Briefly, the pMXs-puro vector carrying cDNAs for EGFP-tagged human ATP8A1, ATP11A, ATP11B, and ATP11C was introduced into HEK293T cells by Fugene 6 (Promega) together with pGag-pol-IRES-bsr, pCMV-VSV-G, and pAdVAntage. The retroviruses produced were concentrated by centrifugation or the Retro-X Concentrator (Clontech) and used to infect W3 mutants. Cells were then cultured in the presence of 1 μg/ml puromycin, and puromycin-resistant cells were subjected to sorting with FACSAria II (BD Biosciences) for the expression of EGFP.

Flippase assay

Flippase activity was assayed as previously described (26, 32). In brief, 2×10^6 cells were incubated with 0.5 μM NBD-PS in 600 μl of HBSS containing 1 mM $MgCl_2$ and 2 mM $CaCl_2$. An aliquot (100 μl) was mixed with 150 μl HBSS containing 5 mg/ml fatty acid-free BSA and analyzed using FACSCanto II (BD Biosciences).

Calcium ionophore treatment and PtdSer exposure

Calcium-induced PtdSer exposure and its return to the intracellular side were analyzed as previously described (30). In brief, 1×10^6 cells were washed with PBS and suspended in 1 ml of annexin V buffer [10 mM Hepes-KOH buffer (pH 7.4) containing 140 mM NaCl and 2.5 mM $CaCl_2$]. After a pre-incubation at 30 °C for 5 to 7 min, cells were treated with 3 μM A23187 at 30 °C for 5 min. Cy5-annexin V and propidium iodide were added to 150-μl aliquots at final concentrations of a 1000-fold dilution and 5 μg/ml, respectively, and analyzed by flow cytometry. After diluting the remaining reaction mixture (850 μl) with 2 to 5 ml of RPMI1640 containing 10% FCS and 2 mM EGTA in the presence or absence of Dyngo-4a, cells were collected by centrifugation and incubated at 15 °C or 37 °C for the indicated time in 1 ml of RPMI1640-10% FCS-2 mM EGTA in the presence or absence of Dyngo-4a. PtdSer on the surface was then analyzed by flow cytometry with Cy5-annexin V as described above.

Transferrin internalization and confocal microscopic analysis

The internalization of the pHrodo-Transferrin conjugate was analyzed as follows. One million cells were placed on ice for 10 min, washed with prechilled imaging buffer (20 mM Hepes buffer, pH 7.4, 140 mM NaCl, 2.5 mM KCl, 1.8 mM $CaCl_2$, 1 mM $MgCl_2$, 20 mM glucose, and 1% BSA), and resuspended in 1 ml of imaging buffer containing 322 nM of the pHrodo-Transferrin conjugate and 3.6 μM of Hoechst 33342, followed by an incubation at 37 °C for 20 min. For PlasMem Bright staining, 1×10^5 cells were collected and resuspended in 100 μl of HBSS containing 2% FCS, 3.6 μM of Hoechst 33342, and 200-fold diluted PlasMem Bright Red.

Cells were then transferred to a glass-bottomed dish, and images were acquired using an LSM 710 confocal laser-scanning microscope (Carl Zeiss).

Purification of the flippase complex and an ATPase assay

The production and purification of the recombinant flippase complex were performed as previously described (26, 37). In brief, using polyethylenimine-mediated transfection (60), the pEF-BOS vector carrying cDNA for Flag-tagged hATP11C, hATP11B, or hATP8A1 was introduced into HEK293T cells together with pEF-BOS-hCDC50A-EGFP. Forty-eight hours after transfection, cells were lysed with solubilization buffer [40 mM Tris buffer (pH 7.5), 5 mM MgCl$_2$, 150 mM NaCl, 10% glycerol, 0.5 mM DTT, 0.5% LMNG, and a mixture of protease inhibitors (Nacalai)]. Cell lysates were applied to anti-FLAG M2-beads, and bound proteins were eluted with elution buffer [40 mM Tris buffer (pH 7.5) containing 150 mM NaCl, 10% glycerol, 0.5 mM DTT, 0.05% LMNG and 160 µg/ml 3×FLAG Peptide (Sigma-Aldrich)].

The ATPase activity of recombinant P4-ATPase was assayed as previously described (26). In brief, 40 µl of reaction buffer [40 mM Tris buffer (pH 7.5), 5 mM MgCl$_2$, 150 mM NaCl, 600 µM ATP, 10% glycerol, 5 mM DTT, and 0.05% LMNG] containing approximately 10 ng of the purified protein was prepared on ice, successively incubated at room temperature for 10 min to warm the solution and at 37 °C for 20 min. Released phosphate was reacted with malachite green oxalate and ammonium heptamolybdate tetrahydrate in the presence of polyvinyl alcohol, and the resulting malachite green–molybdate phosphate complex was detected at 610 nm using a microplate reader (Infinite M200; Tecan).

SDS-PAGE, BN-PAGE, and Western blotting

Regarding SDS-PAGE, the purified flippase complex was incubated at room temperature for 20 min in SDS sample buffer [66 mM Tris-HCl buffer (pH 6.8), 2% SDS, 10% glycerol, 1% β-mercaptoethanol, and 0.003% bromophenol blue] and separated by electrophoresis on a 7.5 or 10% polyacrylamide gel (Nacalai). Precision Plus Protein Standards (Bio-Rad) were used as molecular weight markers.

BN-PAGE was performed according to a previously reported method (61). Briefly, the purified flippase complex in elution buffer was mixed with 1/10 volume of 5% CBB G-250 and loaded onto NativePAGE Novex^R 4 to 16% Bis-Tris Gels (Life Technologies). After electrophoresis at 150 V at 4 °C for 35 min, the concentration of CBB G-250 in the running buffer was changed from 0.02 to 0.002%, and the sample was further electrophoresed at 150 V for 120 min. Protein Standards (Thermo Fisher Scientific), consisting of an IgM hexamer (1236 kDa), IgM pentamer (1048 kDa), apoferritin (720 and 480 kDa), B-phycoerythrin (242 kDa), lactate dehydrogenase (146 kDa), BSA (66 kDa), and soybean trypsin inhibitor (20 kDa), were used as molecular weight markers.

In Western blotting, proteins were transferred to PVDF membranes (Merck Millipore) immediately after SDS-PAGE. BN-PAGE gels were immersed at room temperature for 15 min in SDS loading buffer [25 mM Tris-HCl (pH 8.3), 192 mM glycine, and 0.1% SDS] and transferred to PVDF membranes. Membranes were probed with HRP-anti-FLAG M2 mAb or anti-GFP Ab, followed by detection with Immobilon Western Chemiluminescent HRP substrate (Merck Millipore) or Chemi-Lumi One Super (Nacalai). In some cases, proteins on PVDF membranes were stained with Ponceau S.

Data availability

All data described are located in this article.

Conflict of interest—K. Y. is on a leave of absence from Chugai Pharmaceutical Co.

Abbreviations—The abbreviations used are: P4-ATPase, type IV P-type ATPase; PtdSer, phosphatidylserine; PtdEtn, phosphatidylethanolamine; SM, sphingomyelin; NBD-PS, 1-oleoyl-2-{6-[(7-nitro-2−1,3-benzoxadiazol-4-yl)amino]hexanoyl}-sn-glycero-3-phosphoserine; POPS, 1-palmitoyl-2-oleoyl-sn-glycero-3-phospho-L-serine; POPE, 1-palmitoyl-2-oleoyl-sn-glycero-3-phosphoethanolamine; POPC, 1-palmitoyl-2-oleoyl-glycero-3-phosphocholine; HBSS, Hank's balanced salt solution; CBB, Coomassie Brilliant Blue; LMNG, lauryl maltose-neopentyl glycol; Ab, antibody; HRP, horseradish peroxidase; MFI, median fluorescence intensity.

References

1. Harayama, T., and Riezman, H. (2018) Understanding the diversity of membrane lipid composition. *Nat. Rev. Mol. Cell Biol* **19**, 281–296
2. Yang, Y., Lee, M., and Fairn, G. D. (2018) Phospholipid subcellular localization and dynamics. *J. Biol. Chem.* **293**, 6230–6240
3. van Meer, G., Voelker, D. R., and Feigenson, G. W. (2008) Membrane lipids: where they are and how they behave. *Nat. Rev. Mol. Cell Biol* **9**, 112–124
4. Murate, M., Abe, M., Kasahara, K., Iwabuchi, K., Umeda, M., and Kobayashi, T. (2015) Transbilayer distribution of lipids at nano scale. *J. Cell Sci* **128**, 1627–1638
5. Zhou, Y., and Hancock, J. F. (2021) Lipid profiles of RAS nanoclusters regulate RAS function. *Biomolecules* **11**, 1439

6. Sartorel, E., Unlu, C., Jose, M., Massoni-Laporte, A., Meca, J., Sibarita, J. B., *et al.* (2018) Phosphatidylserine and GTPase activation control Cdc42 nanoclustering to counter dissipative diffusion. *Mol. Biol. Cell* **29**, 1299–1310

7. Lenoir, G., D'Ambrosio, J. M., Dieudonne, T., and Copic, A. (2021) Transport pathways that contribute to the cellular distribution of phosphatidylserine. *Front Cell Dev Biol* **9**, 737907

8. Bevers, E. M., and Williamson, P. L. (2016) Getting to the outer leaflet: physiology of phosphatidylserine exposure at the plasma membrane. *Physiol. Rev.* **96**, 605–645

9. Nagata, S., Sakuragi, T., and Segawa, K. (2020) Flippase and scramblase for phosphatidylserine exposure. *Curr. Opin. Immunol.* **62**, 31–38

10. Segawa, K., and Nagata, S. (2015) An apoptotic 'eat Me' signal: phosphatidylserine exposure. *Trends Cell Biol* **25**, 639–650

11. Nagata, S., and Segawa, K. (2021) Sensing and clearance of apoptotic cells. *Curr. Opin. Immunol.* **68**, 1–8

12. Ryoden, Y., Fujii, T., Segawa, K., and Nagata, S. (2020) Functional expression of the P2X7 ATP receptor requires Eros. *J. Immunol.* **204**, 559–568

13. Bevers, E. M., Tilly, R. H., Senden, J. M., Comfurius, P., and Zwaal, R. F. (1989) Exposure of endogenous phosphatidylserine at the outer surface of stimulated platelets is reversed by restoration of aminophospholipid translocase activity. *Biochemistry* **28**, 2382–2387

14. van den Eijnde, S. M., van den Hoff, M. J., Reutelingsperger, C. P., van Heerde, W. L., Henfling, M. E., Vermeij-Keers, C., *et al.* (2001) Transient expression of phosphatidylserine at cell-cell contact areas is required for myotube formation. *J. Cell Sci* **114**, 3631–3642

15. Das, M., Xu, B., Lin, L., Chakrabarti, S., Shivaswamy, V., and Rote, N. S. (2004) Phosphatidylserine efflux and intercellular fusion in a BeWo model of human villous cytotrophoblast. *Placenta* **25**, 396–407

16. Gadella, B. M., and Harrison, R. A. (2002) Capacitation induces cyclic adenosine 3',5'-monophosphate-dependent, but apoptosis-unrelated, exposure of aminophospholipids at the apical head plasma membrane of boar sperm cells. *Biol. Reprod.* **67**, 340–350

17. Montigny, C., Lyons, J., Champeil, P., Nissen, P., and Lenoir, G. (2016) On the molecular mechanism of flippase- and scramblase-mediated phospholipid transport. *Biochim. Biophys. Acta* **1861**, 767–783

18. Suzuki, J., Umeda, M., Sims, P. J., and Nagata, S. (2010) Calcium-dependent phospholipid scrambling by TMEM16F. *Nature* **468**, 834–838

19. Suzuki, J., Denning, D. P., Imanishi, E., Horvitz, H. R., and Nagata, S. (2013) Xk-related protein 8 and CED-8 promote phosphatidylserine exposure in apoptotic cells. *Science* **341**, 403–406

20. Andersen, J. P., Vestergaard, A. L., Mikkelsen, S. A., Mogensen, L. S., Chalat, M., and Molday, R. S. (2016) P4-ATPases as phospholipid flippases-structure, function, and Enigmas. *Front Physiol.* **7**, 275

21. Tanaka, K., Fujimura-Kamada, K., and Yamamoto, T. (2011) Functions of phospholipid flippases. *J. Biochem.* **149**, 131–143

22. Lee, S., Uchida, Y., Wang, J., Matsudaira, T., Nakagawa, T., Kishimoto, T., *et al.* (2015) Transport through recycling endosomes requires EHD1 recruitment by a phosphatidylserine translocase. *EMBO J.* **34**, 669–688

23. Wang, J., Molday, L. L., Hii, T., Coleman, J. A., Wen, T., Andersen, J. P., *et al.* (2018) Proteomic analysis and functional Characterization of P4-ATPase phospholipid flippases from Murine tissues. *Sci. Rep.* **8**, 10795

24. Cheng, M. T., Chen, Y., Chen, Z. P., Liu, X., Zhang, Z., Chen, Y., *et al.* (2022) Structural insights into the activation of autoinhibited human lipid flippase ATP8B1 upon substrate binding. *Proc. Natl. Acad. Sci. U S A.* **119**, e2118656119

25. Dieudonne, T., Herrera, S. A., Laursen, M. J., Lejeune, M., Stock, C., Slimani, K., *et al.* (2022) Autoinhibition and regulation by phosphoinositides of ATP8B1, a human lipid flippase associated with intrahepatic cholestatic disorders. *Elife* **11**, e75272

26. Segawa, K., Kurata, S., and Nagata, S. (2016) Human type IV P-type ATPases that work as plasma membrane phospholipid flippases and their regulation by caspase and calcium. *J. Biol. Chem.* **291**, 762–772

27. Takatsu, H., Tanaka, G., Segawa, K., Suzuki, J., Nagata, S., Nakayama, K., *et al.* (2014) Phospholipid flippase activities and substrate specificities of human type IV P-type ATPases localized to the plasma membrane. *J. Biol. Chem.* **289**, 33543–33556

28. Takatsu, H., Baba, K., Shima, T., Umino, H., Kato, U., Umeda, M., *et al.* (2011) ATP9B, a P4-ATPase (a putative aminophospholipid translocase), localizes to the trans-Golgi network in a CDC50 protein-independent manner. *J. Biol. Chem.* **286**, 38159–38167

29. Okamoto, S., Naito, T., Shigetomi, R., Kosugi, Y., Nakayama, K., Takatsu, H., *et al.* (2020) The N- or C-terminal cytoplasmic regions of P4-ATPases determine their cellular localization. *Mol. Biol. Cell* **31**, 2115–2124

30. Segawa, K., Yanagihashi, Y., Yamada, K., Suzuki, C., Uchiyama, Y., and Nagata, S. (2018) Phospholipid flippases enable precursor B cells to flee engulfment by macrophages. *Proc. Natl. Acad. Sci. U S A.* **115**, 12212–12217

31. McCluskey, A., Daniel, J. A., Hadzic, G., Chau, N., Clayton, E. L., Mariana, A., *et al.* (2013) Building a better dynasore: the dyngo compounds potently inhibit dynamin and endocytosis. *Traffic* **14**, 1272–1289

32. Segawa, K., Kurata, S., Yanagihashi, Y., Brummelkamp, T. R., Matsuda, F., and Nagata, S. (2014) Caspase-mediated cleavage of phospholipid flippase for apoptotic phosphatidylserine exposure. *Science* **344**, 1164–1168

33. Sullivan, P. C., Ferris, A. L., and Storrie, B. (1987) Effects of temperature, pH elevators, and energy production inhibitors on horseradish peroxidase transport through endocytic vesicles. *J. Cell Physiol* **131**, 58–63

34. Kuismanen, E., and Saraste, J. (1989) Low temperature-induced transport blocks as tools to manipulate membrane traffic. *Methods Cell Biol* **32**, 257–274

35. Takahashi, M., Seino, R., Ezoe, T., Ishiyama, M., and Ueno, Y. (2020) Amphipathic fluorescent dyes for sensitive and long-term Monitoring of plasma membranes. *bioRxiv*. https://doi.org/10.1101/2020.11.16.379206.

36. Ghosh, R. N., Gelman, D. L., and Maxfield, F. R. (1994) Quantification of low density lipoprotein and transferrin endocytic sorting HEp2 cells using confocal microscopy. *J. Cell Sci* **107**, 2177–2189

37. Segawa, K., Kurata, S., and Nagata, S. (2018) The CDC50A extracellular domain is required for forming a functional complex with and chaperoning phospholipid flippases to the plasma membrane. *J. Biol. Chem.* **293**, 2172–2182

38. Tsuchiya, M., Hara, Y., Okuda, M., Itoh, K., Nishioka, R., Shiomi, A., *et al.* (2018) Cell surface flip-flop of phosphatidylserine is critical for PIEZO1-mediated myotube formation. *Nat. Commun.* **9**, 2049

39. Park, J., Choi, Y., Jung, E., Lee, S. H., Sohn, J. W., and Chung, W. S. (2021) Microglial MERTK eliminates phosphatidylserine-displaying inhibitory post-synapses. *EMBO J.* **40**, e107121

40. Grifell-Junyent, M., Baum, J. F., Valimets, S., Herrmann, A., Paulusma, C. C., Lopez-Marques, R. L., *et al.* (2022) CDC50A is required for aminophospholipid transport and cell fusion in mouse C2C12 myoblasts. *J. Cell Sci* **135**, jcs258649

41. Sebastian, T. T., Baldridge, R. D., Xu, P., and Graham, T. R. (2012) Phospholipid flippases: Building asymmetric membranes and transport vesicles. *Biochim. Biophys. Acta* **1821**, 1068–1077

42. Stevens, H. C., Malone, L., and Nichols, J. W. (2008) The putative aminophospholipid translocases, DNF1 and DNF2, are not required for 7-nitrobenz-2-oxa-1,3-diazol-4-yl-phosphatidylserine flip across the plasma membrane of Saccharomyces cerevisiae. *J. Biol. Chem.* **283**, 35060–35069

43. Alder-Baerens, N., Lisman, Q., Luong, L., Pomorski, T., and Holthuis, J. C. (2006) Loss of P4 ATPases Drs2p and Dnf3p disrupts aminophospholipid transport and asymmetry in yeast post-Golgi secretory vesicles. *Mol. Biol. Cell* **17**, 1632–1642

44. Siggs, O. M., Arnold, C. N., Huber, C., Pirie, E., Xia, Y., Lin, P., *et al.* (2011) The P4-type ATPase ATP11C is essential for B lymphopoiesis in adult bone marrow. *Nat. Immunol.* **12**, 434–440

45. Siggs, O. M., Schnabl, B., Webb, B., and Beutler, B. (2011) X-linked cholestasis in mouse due to mutations of the P4-ATPase ATP11C. *Proc. Natl. Acad. Sci. U S A.* **108**, 7890–7895

46. Ochiai, Y., Suzuki, C., Segawa, K., Uchiyama, Y., and Nagata, S. (2022) Inefficient development of syncytiotrophoblasts in the Atp11a-deficient mouse placenta. *Proc. Natl. Acad. Sci. U S A.* **119**, e2200582119

47. Segawa, K., Kikuchi, A., Noji, T., Sugiura, Y., Hiraga, K., Suzuki, C., *et al.* (2021) A sublethal ATP11A mutation associated with neurological

deterioration causes aberrant phosphatidylcholine flipping in plasma membranes. *J. Clin. Invest* **131**, e148005

48. Arashiki, N., Niitsuma, K., Seki, M., Takakuwa, Y., and Nakamura, F. (2019) ATP11C T418N, a gene mutation causing congenital hemolytic anemia, reduces flippase activity due to improper membrane trafficking. *Biochem. Biophys. Res. Commun.* **516**, 705–712

49. Hiraizumi, M., Yamashita, K., Nishizawa, T., and Nureki, O. (2019) Cryo-EM structures capture the transport cycle of the P4-ATPase flippase. *Science* **365**, 1149–1155

50. Nakanishi, H., Irie, K., Segawa, K., Hasegawa, K., Fujiyoshi, Y., Nagata, S., *et al.* (2020) Crystal structure of a human plasma membrane phospholipid flippase. *J. Biol. Chem.* **295**, 10180–10194

51. Hsu, V. W., Bai, M., and Li, J. (2012) Getting active: protein sorting in endocytic recycling. *Nat. Rev. Mol. Cell Biol* **13**, 323–328

52. Chung, J., Torta, F., Masai, K., Lucast, L., Czapla, H., Tanner, L. B., *et al.* (2015) INTRACELLULAR TRANSPORT. PI4P/phosphatidylserine countertransport at ORP5- and ORP8-mediated ER-plasma membrane contacts. *Science* **349**, 428–432

53. Vance, J. E. (2015) Phospholipid synthesis and transport in mammalian cells. *Traffic* **16**, 1–18

54. McCusker, D., and Kellogg, D. R. (2012) Plasma membrane growth during the cell cycle: Unsolved mysteries and recent progress. *Curr. Opin. Cell Biol* **24**, 845–851

55. Atilla-Gokcumen, G. E., Muro, E., Relat-Goberna, J., Sasse, S., Bedigian, A., Coughlin, M. L., *et al*. (2014) Dividing cells regulate their lipid composition and localization. *Cell* **156**, 428–439

56. Ogasawara, J., Watanabe-Fukunaga, R., Adachi, M., Matsuzawa, A., Kasugai, T., Kitamura, Y., *et al*. (1993) Lethal effect of the anti-Fas antibody in mice. *Nature* **364**, 806–809

57. Cong, L., Ran, F. A., Cox, D., Lin, S., Barretto, R., Habib, N., *et al*. (2013) Multiplex genome engineering using CRISPR/Cas systems. *Science* **339**, 819–823

58. Kitamura, T., Koshino, Y., Shibata, F., Oki, T., Nakajima, H., Nosaka, T., *et al*. (2003) Retrovirus-mediated gene transfer and expression cloning: powerful tools in functional genomics. *Exp. Hematol.* **31**, 1007–1014

59. Mizushima, S., and Nagata, S. (1990) pEF-BOS, a powerful mammalian expression vector. *Nucleic Acids Res.* **18**, 5322

60. Raymond, C., Tom, R., Perret, S., Moussouami, P., L'Abbe, D., St-Laurent, G., *et al*. (2011) A simplified polyethylenimine-mediated transfection process for large-scale and high-throughput applications. *Methods* **55**, 44–51

61. Suzuki, J., Imanishi, E., and Nagata, S. (2016) Xkr8 phospholipid scrambling complex in apoptotic phosphatidylserine exposure. *Proc. Natl. Acad. Sci. U S A.* **113**, 9509–9514